Applied and Environmental Microbiology, Feb. 2008, p. 1124–1135 Vol. 74, No. 4
0099-2240/08/$08.00+0 doi:10.1128/AEM.02192-07

Fermentative Utilization of Glycerol by *Escherichia coli* and Its Implications for the Production of Fuels and Chemicals[▽]

Abhishek Murarka,† Yandi Dharmadi,† Syed Shams Yazdani, and Ramon Gonzalez*

Department of Chemical and Biomolecular Engineering, Rice University, P.O. Box 1892, Houston, Texas 77251-1892

Received 26 September 2007/Accepted 10 December 2007

Availability, low prices, and a high degree of reduction make glycerol an ideal feedstock to produce reduced chemicals and fuels via anaerobic fermentation. Although glycerol metabolism in *Escherichia coli* had been thought to be restricted to respiratory conditions, we report here the utilization of this carbon source in the absence of electron acceptors. Cells grew fermentatively on glycerol and exhibited exponential growth at a maximum specific growth rate of 0.040 ± 0.003 h^{-1}. The fermentative nature of glycerol metabolism was demonstrated through studies in which cell growth and glycerol utilization were observed despite blocking several respiratory processes. The incorporation of glycerol in cellular biomass was also investigated via nuclear magnetic resonance analysis of cultures in which either 50% U-^{13}C-labeled or 100% unlabeled glycerol was used. These studies demonstrated that about 20% of the carbon incorporated into the protein fraction of biomass originated from glycerol. The use of U-^{13}C-labeled glycerol also allowed the unambiguous identification of ethanol and succinic, acetic, and formic acids as the products of glycerol fermentation. The synthesis of ethanol was identified as a metabolic determinant of glycerol fermentation; this pathway fulfills energy requirements by generating, in a redox-balanced manner, 1 mol of ATP per mol of glycerol converted to ethanol. A fermentation balance analysis revealed an excellent closure of both carbon (~95%) and redox (~96%) balances. On the other hand, cultivation conditions that prevent H_2 accumulation were shown to be an environmental determinant of glycerol fermentation. The negative effect of H_2 is related to its metabolic recycling, which in turn generates an unfavorable internal redox state. The implications of our findings for the production of reduced chemicals and fuels were illustrated by coproducing ethanol plus formic acid and ethanol plus hydrogen from glycerol at yields approaching their theoretical maximum.

Glycerol has become an inexpensive and abundant carbon source due to its generation as an inevitable by-product of biodiesel fuel production. With every 100 lb of biodiesel produced by transesterification of vegetable oils or animal fats, 10 lb of crude glycerol is generated (38). The tremendous growth of the biodiesel industry has created a glycerol surplus that resulted in a dramatic 10-fold decrease in crude glycerol prices over the last 2 years (38). This decrease in prices represents a problem for the glycerol-producing and -refining industries, and the economic viability of the biodiesel industry itself has been greatly affected (16, 17, 38). Clearly, the development of processes to convert crude glycerol into higher-value products is an urgent need. The use of glycerol as feedstock in fermentation processes has yet another advantage: i.e., given the highly reduced nature of carbon atoms in glycerol, fuels and reduced chemicals can be produced from it at higher yields than those obtained from common sugars such as glucose or xylose (38). To fully realize these advantages, the use of anaerobic fermentations is highly desirable.

Although many microorganisms are able to metabolize glycerol in the presence of external electron acceptors (respiratory metabolism), few are able to do so fermentatively (i.e., absence of electron acceptors). Fermentative metabolism of glycerol has been reported in species of the genera *Klebsiella*, *Citrobacter*, *Enterobacter*, *Clostridium*, *Lactobacillus*, *Bacillus*, *Propionibacterium*, and *Anaerobiospirillum* (see reference 38 and references cited therein). However, the potential for using these organisms at the industrial level could be limited due to issues that include pathogenicity, requirement of strict anaerobic conditions, need of supplementation with rich nutrients, and unavailability of the genetic tools and physiological knowledge necessary for their effective manipulation. The use of microbes such as *Escherichia coli*, an organism very amenable to industrial applications, could help overcome the aforementioned problems. Metabolism of glycerol in *E. coli*, however, has been thought for many years to require the presence of external electron acceptors (2, 15, 24, 25). The respiratory pathways mediating this metabolic process involve a glycerol transporter (encoded by *glpF*), a glycerol kinase (encoded by *glpK*), and two respiratory glycerol-3-phosphate dehydrogenases (G3PDHs), the latter encoded by the *glpD* and *glpABC* operons (3, 22, 31, 36) (Fig. 1).

Unlike previous reports, recent studies in our laboratory indicate that *E. coli* can anaerobically ferment glycerol (7). Our findings represent a promising solution to the aforementioned problems as they could facilitate the development of *E. coli*-based platforms to convert low-value raw glycerol to higher-value reduced chemicals and fuels at yields higher than those obtained from common sugars (38). Since in our previous study we reported that glycerol fermentation in *E. coli* requires the supplementation of the medium with rich nutrients (7), part of this study focuses on demonstrating the fermentative nature of the process and the use of glycerol in the synthesis of

* Corresponding author. Mailing address: Department of Chemical and Biomolecular Engineering, Rice University, 6100 Main Street, MS-362, Houston, TX 77005. Phone: (713) 348-4893. Fax: (713) 348-5478. E-mail: ramon.gonzalez@rice.edu.

† A.M. and Y.D. contributed equally to this work.

▽ Published ahead of print on 21 December 2007.

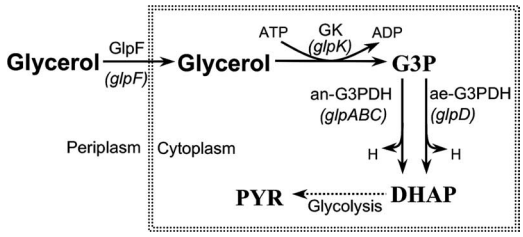

FIG. 1. Respiratory metabolism of glycerol in *E. coli*. Glycerol dissimilation in the presence of electron acceptors is mediated by an ATP-dependent glycerol kinase (GK, coded for by *glpK*) and two respiratory G3PDHs (aerobic and anaerobic enzymes, encoded by *glpD* and *glpABC*, respectively). Abbreviations: DHAP, dihydroxyacetone phosphate; GK, glycerol kinase; ae-G3PDH, aerobic G3PDH; H, reducing equivalents (H = NADH/NADPH/$FADH_2$); PYR, pyruvate.

cell mass. We also investigate here the role of the main fermentative pathways, the effect of cultivation conditions such as pH, and the nature of the gas atmosphere and illustrate the usefulness of our findings through the coproduction of ethanol and formic acid and ethanol and hydrogen from glycerol.

MATERIALS AND METHODS

Strains, plasmids, and genetic methods. Wild-type *E. coli* strains MC4100 (ATCC 35695), W3110 (ATCC 27325), and B (ATCC 11303) were obtained from the American Type Culture Collection (ATCC, Manassas, VA). K-12 strain MG1655 (F^- λ^- *ilvG rfb-50 rph-1*) and the following otherwise isogenic derivatives were obtained from the University of Wisconsin *E. coli* Genome Project (www.genome.wisc.edu): FB21196 (*glpD*::Tn*5*KAN-I-SceI), FB20724 (*glpA*::Tn*5*KAN-I-SceI), FB21553 (*glpK*::Tn*5*KAN-I-SceI), FB20272 (*adhE*::Tn*5*KAN-I-SceI), FB20752 (*pta*::Tn*5*KAN-I-SceI), FB21716 (*frdA*::Tn*5*KAN-I-SceI), FB20228 (*cydA*::Tn*5*KAN-I-SceI), FB20172 (*cyoB*::Tn*5*KAN-I-SceI), FB23319 (*fixA*::Tn*5*KAN-I-SceI), and FB20908 (*hycB*::Tn*5*KAN-I-SceI). These strains carry a transposon (Tn*5*) insertion mutation in the specified gene (12). Plasmid pCA24N (referred to here as pCA24NAdhE) expressing the gene *adhE* from the IPTG (isopropyl-β-D-thiogalactopyranoside)-inducible promoter pT5/lac (14) was used in complementation studies. pCA24NAdhE was obtained from the Genome Analysis Project Japan (http://ecoli.aist-nara.ac.jp/), transformed into *E. coli* strains, and selected on Luria-Bertani (LB) plates supplemented with 34 μg/ml chloramphenicol. Gene expression was induced with 10 μM IPTG. Standard recombinant DNA procedures were used for plasmid isolation and electroporation (26). The strains were kept in 32.5% glycerol stocks at −80°C. Plates were prepared using LB medium containing 1.5% agar, and appropriate antibiotics were included as needed at the following concentrations: 34 μg/ml chloramphenicol and 50 μg/ml kanamycin.

Culture medium and cultivation conditions. The minimal medium (MM) designed by Neidhardt et al. (18) supplemented with 2 g/liter tryptone (Difco), 5 μM sodium selenite, 1.32 mM Na_2HPO_4 in place of K_2HPO_4, and 110 mM of glycerol was used, unless otherwise specified. MOPS (morpholinopropanesulfonic acid) was only included in the inoculum preparation phase or in experiments conducted in tubes (see below). Chemicals were obtained from Fisher Scientific (Pittsburgh, PA) and Sigma-Aldrich Co. (St. Louis, MO).

Fermentations were conducted in a SixFors multifermentation system (Infors HT, Bottmingen, Switzerland) with six 500-ml-working-volume vessels and independent control of temperature (37°C), pH, and stirrer speed (200 rpm) (7). The system is fully equipped and computer controlled using the manufacturer's IRIS NT software. Each vessel is fitted with a condenser to minimize evaporation, which was operated with a 0°C cooling methanol-water supply. Anaerobic conditions were maintained by initially sparging the medium with ultra-high-purity argon (Matheson, Tri-Gas, Houston, TX) and thereafter flushing the headspace with the same gas at 0.01 liter per min. An oxygen trap (Alltech Associates, Inc., Deerfield, IL) was used to eliminate traces of oxygen from the gas stream. In some experiments (specified in each case), carbon dioxide or hydrogen was also included in the gas phase. An experiment designed to assess the incorporation of glycerol into proteinogenic amino acids in cell mass was conducted using 17-ml Hungate tubes (Bellco Glass, Inc., Vineland, NJ), which were modified by piercing the septa with two Luer lock needles—one for oxygen-free argon sparging (20G × 2 in.; Hamilton Company-USA, Reno, NV) and one for gas efflux (20G × 8 in.; Hamilton Company-USA, Reno, NV). Mixing was achieved through the rising gas bubbles. The working volume of these modified Hungate tubes was 10 ml.

Prior to use, the cultures (stored as glycerol stocks at −80°C) were streaked onto LB plates and incubated overnight at 37°C in an Oxoid anaerobic jar with the CO_2 gas-generating kit (Oxoid Ltd., Basingstoke, Hampshire, United Kingdom). A single colony was used to inoculate 17.5-ml Hungate tubes completely filled with medium (MM supplemented with 10 g/liter tryptone, 5 g/liter yeast extract, and 5 g/liter glycerol). The tubes were incubated at 37°C until an optical density at 550 nm (OD_{550}) of ~0.4 was reached. An appropriate volume of this actively growing preculture was centrifuged, and the pellet was washed and used to inoculate 350 ml of medium in each fermentor, with the target starting OD_{550} of 0.05.

Analytical methods. OD_{550} was measured and used as an estimate of cell mass (1 OD unit = 0.34 g [dry weight]/liter). After centrifugation, the supernatant was stored at −20°C for high-performance liquid chromatography (HPLC) and nuclear magnetic resonance (NMR) analysis (described in the next section). Glycerol, organic acids, ethanol, and hydrogen were quantified as previously described (7, 8).

NMR experiments. The identity of the fermentation products was determined through NMR experiments. Sixty microliters of D_2O and 1 μl of 600 mM NMR internal standard TSP [3-(trimethylsilyl) propionic acid-D4, sodium salt] were added to 540 μl of the sample (culture supernatant). The resulting solution was then transferred to a 5 mm-NMR tube, and 1D proton NMR spectroscopy was performed at 25°C in a Varian 500-MHz Inova spectrometer equipped with a Penta probe (Varian, Inc., Palo Alto, CA). The following parameters were used: 8,000-Hz sweep width, 2.8-s acquisition time, 256 acquisitions, 6.3-μs pulse width, 1.2-s pulse repetition delay, and presaturation for 2 s. The resulting spectrum was analyzed using FELIX 2001 software (Accelrys Software Inc., Burlington, MA). Peaks were identified by their chemical shifts and J-coupling values, which were obtained in separate experiments in which samples were spiked with metabolite standards (2 mM final concentration).

An experiment with 50% U-^{13}C-labeled glycerol was conducted to assess the incorporation of glycerol into proteinogenic biomass and to verify that fermentation products originate from glycerol and not from tryptone components. These experiments were conducted using modified Hungate tubes as described in the section "Culture medium and cultivation conditions." After 72 h, cultures were harvested and the fermentation broth was centrifuged. The cell pellets were washed twice with 9 g/liter NaCl solution and centrifuged again. The resulting cell pellets were hydrolyzed with 6 N constantly boiling HCl at 110°C for 24 h using the Reacti-Therm hydrolysis system (Pierce, Rockford, IL). To remove HCl, the resulting solutions were subjected to rapid vaporization at 75°C under vacuum for 2 h using the CentriVap system (Labconco Corp., Kansas City, MO). The dried samples were reconstituted in 1 ml D_2O (Cambridge Isotope Laboratories, Cambridge, MA), frozen to −80°C, and subsequently freeze-dried in the 4.5-liter FreeZone freeze-dry system (Labconco Corp., Kansas City, MO) for 24 h. The samples were then reconstituted in 600 μl D_2O and filtered to remove cell particulates. One microliter of TSP standard was added to each sample, and the contents were transferred to NMR tubes. To determine ^{13}C enrichment, the samples were analyzed using 1D proton spin echo with and without concurrent 90° pulse on carbon (1). The 90° pulse on carbon refocused the ^{13}C carbon atoms, thereby suppressing the ^{13}C satellites arising due to proton-carbon spin coupling. This phenomenon did not occur for the ^{12}C carbon atoms. For these experiments, we used the commercially available pulse sequence *pwxcal* on a 500-MHz Varian Innova spectrometer (Varian, Inc., Palo Alto, CA). The following parameters were used: 8,000-Hz sweep width, 2.7-s acquisition time, 256 transients, and pwx1 of 0 and 90° at 25°C. Individual amino acids were identified based on chemical shifts and the fine structure of the spectra (9). 1D proton NMR spectroscopy, performed as described above, was also used to analyze the supernatant of the 72-h culture to assess whether the fermentation products were synthesized from glycerol or tryptone components. The sample preparation and acquisition parameters were those described above for the analysis of fermentation broth through 1D ^{1}H NMR spectroscopy.

Enzyme activities. For enzyme assays, cells were grown on MOPS medium (see above) supplemented with 10 g/liter glycerol, 5 g/liter yeast extract, and 10 g/liter tryptone. Cells were harvested in the late log phase of growth, washed, resuspended in 0.1 M potassium phosphate buffer, and permeabilized with chloroform (20, 33). For the aerobic G3PDH (a-G3PDH) assay, the cells were grown aerobically. For the anaerobic G3PDH (an-G3PDH) assay, on the other hand, cells were grown anaerobically in the presence of 20 mM fumarate. The assay for measuring an-G3PDH activity is a modification of the assay described by Kistler

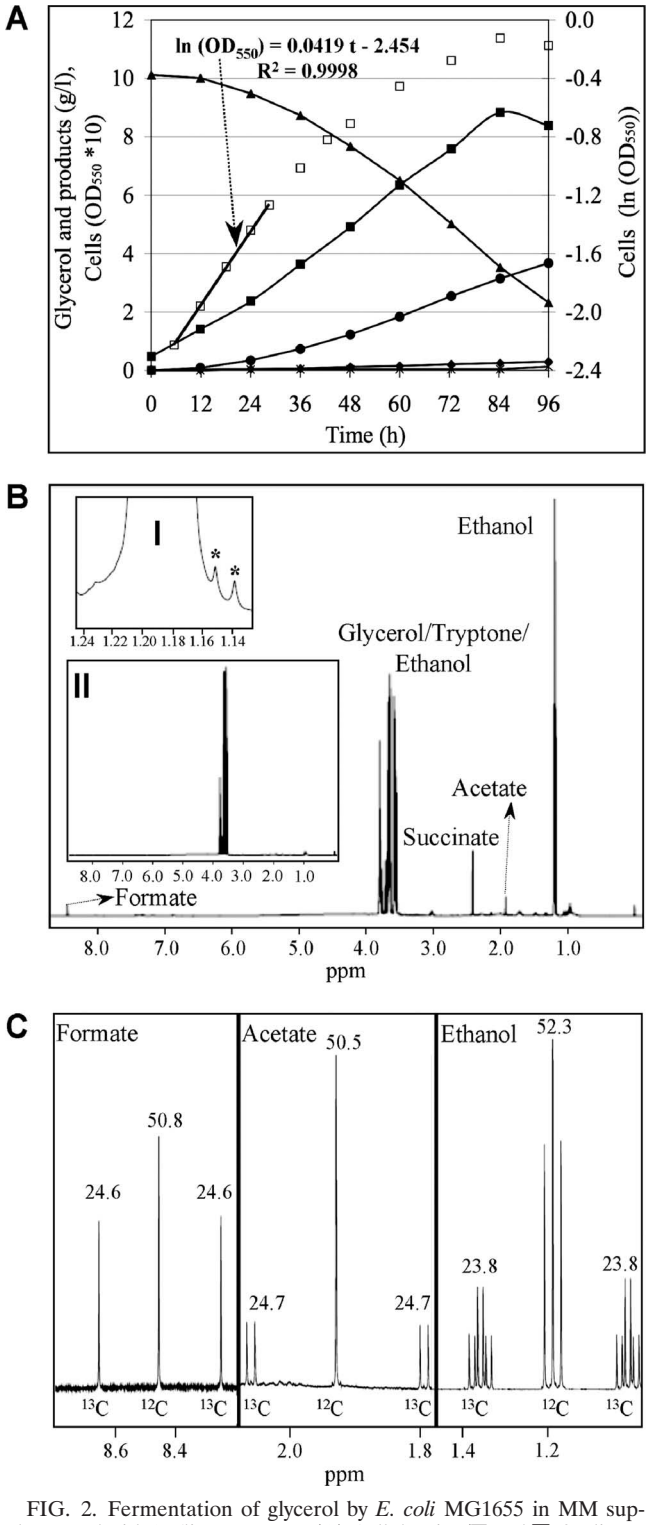

FIG. 2. Fermentation of glycerol by *E. coli* MG1655 in MM supplemented with 2 g/liter tryptone. (A) Cell density (■ and □, for linear and log-linear plots, respectively) and concentrations of glycerol (▲), ethanol (●), succinic acid (◆), and formic plus acetic acids (×). Additional measurements of OD taken during the exponential growth phase are shown in the log-linear plot, along with their fitting to a straight-line model (least-squares method). (B) 1D ^{1}H NMR spectrum of the culture medium in a late fermentation sample. (Inset I) Two peaks at the same chemical shifts as those of methyl protons of 1,2-PDO (doublet at 1.15 ppm) are shown (*). (Inset II) Spectra for the time zero sample. (C) 1D ^{1}H NMR spectra of the fermentation broth from a 72-h culture grown on a mixture of 50% U-^{13}C-labeled and 50% unlabeled glycerol. The percentage of area of each peak to that of total area (i.e., sum of all peaks) is shown.

and Lin (13), utilizing the following final concentrations: 3-(4,5-dimethyl-2-thiazolyl)-2,5-diphenyl-2H-tetrazolium bromide (MTT), 75 μM; phenazine methosulfate, 600 μM; DL-glycerol 3-phosphate, 10 mM; Triton X-100, 0.2%; flavin adenine dinucleotide (FAD), 10 μM; and flavin mononucleotide (FMN), 1 mM. The a-G3PDH activity was determined in the same way, except that flavins were omitted and sodium cyanide (10 μM) was included in the assay. The assays were monitored spectrophotometrically at 570 nm. The extinction coefficient of reduced MTT was 17 mM^{-1} cm^{-1}. Linearity of reactions (protein concentration and time) was established for all preparations. The nonenzymatic rates were subtracted from the observed initial reaction rates. Results are expressed as μmol of substrate/min/mg of cell protein and are averages for at least three cell preparations.

NADH/NAD$^+$ assay. Intracellular levels of NADH and NAD$^+$ were measured via HPLC as previously described (32). The fermentation broth was collected and centrifuged at 3,200 × *g* for 10 min. For nucleotide extraction, the cell pellet was resuspended in 1 ml of ice-cold 0.5 M KOH and kept on ice for 10 min with intermittent vortexing. This biomass cocktail was centrifuged for 10 min, and 1 ml of 1 M KH_2PO_4 buffer (pH 6.5) was added to the supernatant. The resulting solution was filtered through a 0.22-μm syringe filter, and 100 μl was analyzed via HPLC (Spectra System, Thermo Separation Products, Waltham, MA) with SupelcosilTMLC-18-T column (Supelco, Bellefonte, PA). The samples were run with two different mobile phases indicating two stages of run: inorganic and organic. A 0.1 M concentration of KH_2PO_4 buffer (pH 6) was used during the inorganic stage, and after 20 min, the mobile phase was switched to a mixture of 90% 0.1 M KH_2PO_4 buffer (pH 6) and 10% methanol. The resulting chromatogram was analyzed using the software Chromquest 4.1 (Thermo Electron, Waltham, MA) to obtain the area of peaks corresponding to concentrations of NADH and NAD$^+$. Additional samples spiked with nucleotides were analyzed to verify the identity of the peaks.

Calculation of kinetic parameters. Maximum specific growth rates (μ_M; h^{-1}) were estimated by plotting total cell concentration versus time in a log-linear plot. The slope of the curves thus obtained (a straight line during exponential growth) was used as the average specific rate. Growth yield ($Y_{X/S}$; mg cell/g glycerol) was calculated as the increase in cell mass per glycerol consumed once the cultures reached the stationary phase.

RESULTS

Anaerobic fermentation of glycerol by *E. coli* K-12 and B strains in a low-supplement medium. Our recent studies of glycerol metabolism in *E. coli* indicate that this organism is able to metabolize glycerol in the absence of electron acceptors (7). To further investigate this metabolic process, we conducted studies in which a low-supplement medium is used, namely supplementation with 0.3 to 2 g/liter tryptone instead of 10 g/liter tryptone and 5 g/liter yeast extract in the previous study (7). Figure 2A shows a typical fermentation profile for wild-type strain MG1655 in a medium supplemented with 2 g/liter tryptone. Exponential growth was observed for a period of 24 h, starting when the culture was about 6 h and ending around 30 h (Fig. 2A [note the excellent fitting to a straight-line model in the log-linear plot between 6 and 30 h]). The μ_M during exponential growth for the profile shown in Fig. 2A was 0.0419 h^{-1}: the average μ_M of four fermentations was 0.040 ± 0.003 h^{-1}. Approximately 2 g/liter of glycerol was left unfermented in the medium of stationary-phase cultures (e.g., Fig. 2A). It is noteworthy that no cell growth was observed when glycerol was omitted from the medium formulation (OD increased by less than 0.05).

TABLE 1. Calculation of the fermentation balance for growth of *E. coli* MG1655 on glycerol at pH 6.3 and 37°C

Substrate consumed and products formed	Mol of product/mol of glycerol[a]	Oxidation state[b]	Redox balance[c]	Carbon recovery (no. of C atoms)[d]
Glycerol substrate		−2.0	−2.0	3.0
Products				
Acetic acid	0.012	0.0		0.023
Succinic acid	0.015	+2.0	+0.030	0.060
Carbon dioxide	0.905	+4.0	+3.620	0.905
Hydrogen	0.935	−2.0	−1.870	
Ethanol	0.923	−4.0	−3.692	1.846
Total			−1.912	2.834

[a] Values are net mol produced per mol of glycerol fermented. Since 50% of the succinic acid originated from glycerol, the value shown is half of the amount detected in the fermentation broth. The amounts of formic acid and 1,2-PDO were undetectable via HPLC and therefore not included in this analysis.

[b] The oxidation state of carbon atoms was calculated assuming oxidation states of −2 and +1 for oxygen and hydrogen, respectively (28).

[c] Data in this column were obtained as (mol of product/mol of glycerol) × oxidation state of carbon atoms.

[d] Carbon recovery was calculated as (mol of product/mol of glycerol) × no. of carbon atoms in molecule.

TABLE 2. Glycerol fermentation by *E. coli* K-12 and B strains

Strain	Mean ± SD result for parameter[a]:	
	μ_M (h^{-1})	$Y_{x/S}$ (mg cell/g glycerol)
MG1655	0.040 ± 0.003	32.9 ± 2.9
W3110	0.031 ± 0.002	32.2 ± 3.1
MC4100	0.029 ± 0.004	54.9 ± 8.8
B	0.036 ± 0.002	34.1 ± 2.7

[a] μ_M, maximum specific growth rate calculated during exponential growth; $Y_{x/S}$, growth yield calculated as the increase in cell mass per glycerol consumed once the cultures reached stationary phase.

The identity of the fermentation products was determined through 1D ^{1}H (proton) NMR spectroscopy analysis of the extracellular media. Fermentation products identified include ethanol (two multiplets at 3.66 and 1.19 ppm) and the following organic acids: succinic acid (2.444 ppm), acetic acid (1.93 ppm), and formic acid (8.46 ppm) (Fig. 2B). No lactic acid was detected in the extracellular medium. A doublet was observed in the spectra of late fermentation samples at a position with the same chemical shift as that of methyl protons of 1,2-propanediol (1,2-PDO) (doublet at 1.15 ppm: Fig. 2B, inset I). These results indicate that *E. coli* has the ability to produce 1,2-PDO as a product of glycerol fermentation. The concentration of glycerol and products identified in the NMR spectrum were determined via HPLC, with the exception of 1,2-PDO, which was quantified via NMR and by using TSP as an internal standard. We found that about 0.5 ± 0.15 mM 1,2-PDO is present in stationary-phase samples from the culture shown in Fig. 2A.

We conducted a separate experiment to verify that the products identified above were in fact synthesized from glycerol and not from tryptone components. To this end, cells were grown on a mixture of 50% U-^{13}C-labeled and 50% unlabeled glycerol (10 g/liter of glycerol total). Selected areas of the NMR spectrum of the supernatant of a 72-h sample from this culture are shown in Fig. 2C. 1D ^{1}H NMR spectroscopy was used in these experiments to distinguish between ^{13}C and ^{12}C atoms (see Materials and Methods for more details). Since ^{13}C is magnetic, protons attached to ^{13}C carbons have two different chemical shifts due to the positive and negative energy levels of these carbon atoms. Protons attached to ^{12}C atoms will have chemical shifts in between those of ^{13}C because all ^{12}C atoms will be at a neutral state. Thus, protons attached to ^{12}C carbon atoms lead to a central peak structure flanked by two satellite peak structures that arise from those protons attached to the ^{13}C atoms. The percentage area of ^{13}C satellite peaks to that of total area would then reflect the ^{13}C enrichment of that carbon atom. As can be seen from Fig. 2C, the ^{13}C enrichment in ethanol and acetic and formic acids is almost identical to the fraction of U-^{13}C-labeled glycerol used in the experiment (~50%), demonstrating that all carbon atoms in these products originated from glycerol. ^{13}C enrichment was also observed in the case of succinic acid, although the value was about half of that observed for the other products (data not shown).

The quantification of fermentation products allowed the performance of a fermentation balance analysis, which is presented in Table 1. The carbon recovered as fermentation products represents approximately 95% of the carbon consumed as glycerol (2.834/3 = 0.945; see Table 1). Similarly, about 96% of the reducing equivalents generated during the fermentation of glycerol were captured in the synthesis of fermentation products (−1.912/−2 = 0.956; see Table 1). This analysis demonstrates an excellent closure of redox and carbon balances, both reaching levels similar to those reported for the fermentative metabolism of other carbon sources such as glucose (28).

Since different *E. coli* strains vary significantly in their genotype and metabolic capabilities (21, 23), we investigated whether glycerol fermentation was feasible in other commonly used strains. Like MG1655, K-12 strains W3110 and MC4100 and *E. coli* strain B were all able to ferment glycerol (Table 2). Cell growth and glycerol utilization by these strains were also observed when the medium was supplemented with lower levels of tryptone. For example, MG1655 grew to an OD_{550} of 0.53 and fermented 9 g/liter of glycerol in a medium supplemented with 0.3 g/liter of tryptone. Similar results were achieved by supplementing the medium with a mixture of proteinogenic amino acids at levels similar to those provided by the tryptone supplementation: i.e., an OD_{550} of 0.6 and 8.9 g/liter of glycerol fermented were achieved. However, the use of the aforementioned levels of tryptone or amino acid supplementation resulted in lower cell density and slower fermentation kinetics than those shown in Fig. 2A. Since we did not observe glycerol fermentation in the absence of supplementation, we conducted experiments to demonstrate that: (i) glycerol is used in the synthesis of cell mass and (ii) tryptone is not a source of electron acceptors. Our results are discussed in the next two sections.

Use of glycerol in the synthesis of cell mass. To investigate whether glycerol is used in the synthesis of cell mass, we conducted an experiment in which the ^{13}C enrichment of proteinogenic biomass was assessed by using U-^{13}C-labeled glycerol in a medium formulation with 2 g/liter of tryptone. ^{13}C enrichment of biomass in cells grown on a mixture of 50% U-^{13}C-

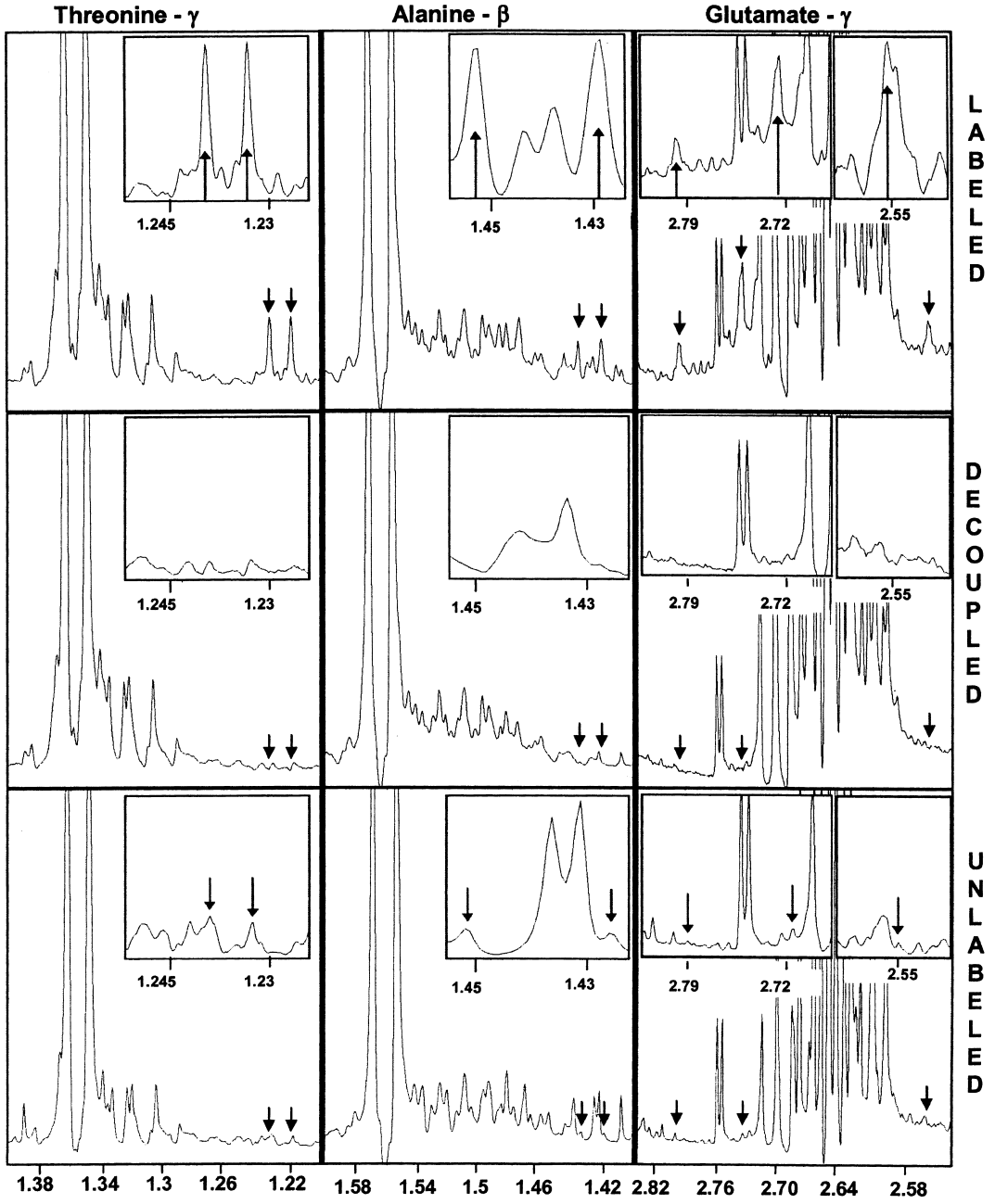

FIG. 3. NMR spectra of proteinogenic amino acids in cell biomass obtained from experiments with 50% U-^{13}C-labeled (top panels) and unlabeled (bottom panels) glycerol. The identity of ^{13}C satellites as peaks arising due to labeled carbon was confirmed by performing a ^{13}C-decoupled experiment in which the ^{13}C signals were suppressed (middle panels). Marked peaks (arrows) illustrate the incorporation of labeled carbon into threonine-γ (left panels), alanine-β (center panels), and glutamate-γ (right panels). Peaks in bottom panels (unlabeled glycerol) correspond to the natural abundance of ^{13}C.

labeled and 50% unlabeled glycerol (10 g/liter of glycerol total) were compared to a reference culture in which cells were grown on 100% unlabeled glycerol. The cells from the two cultures were hydrolyzed to obtain a cocktail of their proteinogenic amino acids, which was subsequently analyzed via NMR. To determine their ^{13}C enrichment, the samples were analyzed using 1D proton spin echo with and without concurrent 90° pulse on carbon as described in Materials and Methods. The 90° pulse on carbon refocuses the ^{13}C carbon atoms, thereby suppressing the ^{13}C satellites arising due to proton-carbon spin coupling. The nucleus of ^{12}C is nonmagnetic, and thus protons attached to ^{12}C would not experience any difference between the two situations. Therefore, ^{13}C satellite peaks could be easily identified upon comparison of spectra obtained via these two methods. The 1D NMR spectra thus obtained for the two samples (with and without labeled carbon) contained small ^{13}C satellite peaks, which in several cases were hidden below bigger peaks. However, many of them were well resolved with visible

TABLE 3. Cellular response (cell growth) to perturbations in respiratory and fermentative pathways

Condition and strain[a]	Mean ± SD result for parameter[b]:	
	μ_M (h^{-1})	$Y_{X/S}$ (mg cell/g glycerol)
Wild type under reference conditions		
MG1655	0.040 ± 0.003	32.9 ± 2.9
Perturbation of general respiratory processes		
Δ*cydA*	0.030 ± 0.001	30.5 ± 1.2
Δ*cyoB*	0.050 ± 0.004	30.2 ± 1.5
MG1655 + 0.5 mM NaCN	0.019 ± 0.002	40.2 ± 1.6
MG1655 + 0.5 mM NaN_3	0.027 ± 0.002	28.0 ± 1.1
Disruption of specific respiratory processes		
Δ*frdA*	0.057 ± 0.005	29.2 ± 1.7
Δ*fixA*	0.035 ± 0.002	32.0 ± 1.3
Δ*glpA*	0.036 ± 0.002	30.0 ± 1.2
Δ*glpD*	0.040 ± 0.002	35.6 ± 1.4
Δ*glpK*	0.033 ± 0.007	53.4 ± 2.5
Disruption of fermentative pathways		
Δ*pta*	0.029 ± 0.002	26.5 ± 1.6
Δ*adhE*	No growth	No growth
Δ*adhE* (*adhE*$^+$)[c]	0.036 ± 0.003	42.9 ± 2.9

[a] See text for details of products encoded by disrupted genes, evidence that supports the inactivation of encoded activities/functions, and culture conditions.
[b] μ_M is the maximum specific growth rate calculated during exponential growth, and $Y_{X/S}$ is the growth yield calculated once the cells reached stationary phase.
[c] The Δ*adhE* (*adhE*$^+$) strain expresses AdhE from the IPTG-inducible pT5/lac promoter of plasmid pCA24NAdhE. Expression was induced with 10 μM IPTG.

^{13}C satellites. Parts of the NMR spectra depicting three of these resolved areas for each sample are shown in Fig. 3. The depicted amino acid carbon atoms are threonine-γ (left panels), alanine-β (center panels), and glutamate-γ (right panels); the down arrows point to the ^{13}C satellites for these carbon atoms. Each panel contains an inset that magnifies the region of the spectra corresponding to the ^{13}C satellite signals and which also includes arrows that indicate the peaks of interest. Since the signals for these satellites were small, their identity (as peaks arising due to labeled carbon) was confirmed by performing a ^{13}C-decoupled experiment in which the ^{13}C signals were suppressed (Fig. 3, middle panels). In the case of unlabeled glycerol (Fig. 3, bottom panels), the ^{13}C satellite peaks constituted about 1% of the total signal, which represents the natural abundance of this isotope. However, when a mixture of 50% ^{13}C-labeled and unlabeled carbon was used (Fig. 3, top panels), the ^{13}C satellites constituted about 11% of the total signal, indicating that about 20% of these amino acids in biomass originated from glycerol. Although not shown here due to space limitations, similar spectra were obtained for many other carbons corresponding to amino acids in proteinogenic biomass.

Fermentative nature of glycerol metabolism. The requirement of tryptone supplementation also raises questions related to the fermentative nature of glycerol utilization: i.e., could compounds present in the tryptone, or generated from it, serve as electron acceptors? We used several genetic and biochemical strategies to provide conclusive evidence of the fermentative nature of glycerol metabolism, and the results are summarized in Table 3. Glycerol fermentation was still observed in mutant strains devoid of genes encoding members of the aerobic respiratory chain (Δ*cydA* and Δ*cyoB*) and when respiratory inhibitors cyanide and azide were added to the culture medium of wild-type MG1655 (Table 3). While these strategies blocked general respiratory processes, we also evaluated the effect of blocking more specific respiratory events that could potentially take place in the presence of tryptone. For example, fumarate and related C_4 dicarboxylates can be present in the tryptone or generated from some of its components through processes such as the degradation of amino acids. These compounds could then serve as electron acceptors in the respiratory metabolism of glycerol (34). Since these respiratory processes require an active fumarate reductase (FRD), we eliminated this activity by disrupting the gene *frdA*, which encodes a subunit of FRD. The Δ*frdA* mutant produced negligible amounts of succinate, demonstrating the efficiency of the mutation, but did ferment glycerol in a wild-type manner (Table 3). Carnitine is another compound that, if present or generated from tryptone components, can serve as electron acceptor. Since it is well established that *fixA* and *fixB* mutants are unable to perform carnitine respiration (35), we tested a Δ*fixA* mutant and demonstrated that its phenotype was indistinguishable from wild-type MG1655 (Table 3).

TABLE 4. a-G3PDH and an-G3PDH activities

Strain	Mean ± SD activity measured[a]		Growth and glycerol metabolism[b]	
	a-G3PDH	an-G3PDH	Aerobic respiration	Fumarate respiration
Wild type	0.190 ± 0.023	0.072 ± 0.011	+	+
Δ*glpD*	0.001 ± 0.0002	NT	−	+
Δ*glpA*	NT	0.008 ± 0.001	+	−

[a] All activities (in μmol of glycerol/min/mg of cell protein) were measured in MM supplemented with 10 g/liter glycerol, 10 g/liter tryptone, and 5 g/liter yeast extract. Cells were grown aerobically or anaerobically as indicated in each assay. For the anaerobic assay, cells were grown in the presence of 20 mM fumarate. Reported values are averages ± standard deviation of triplicate assays. NT, not tested.
[b] Growth was tested in MM supplemented with 10 g/liter of glycerol under aerobic or anaerobic conditions, as indicated. A 20 mM concentration of fumarate was added to test cell growth via fumarate respiration under anaerobic conditions.

The respiratory metabolism of glycerol in *E. coli* has been studied for many years, and it is a well-characterized metabolic process (2). In the absence of oxygen and presence of other electron acceptors, a three-subunit enzyme that converts glycerol-3-phosphate (G3P) into dihydroxyacetone-phosphate (an-G3PDH) is responsible for the respiratory metabolism of glycerol (2) (Fig. 1). We now demonstrate that a mutant devoid of gene *glpA*, which is required for the activity of an-G3PDH, was able to grow on and ferment glycerol (Table 3). an-G3PDH activity in the Δ*glpA* mutant was negligible compared to its wild-type value (Table 4). Since *glpA*-encoded an-G3PDH activity is known to be required for the anaerobic metabolism of glycerol in the presence of fumarate (2), we tested wild-type and Δ*glpA* mutant strains for their ability to metabolize glycerol via fumarate respiration. Unlike wild-type MG1655, the Δ*glpA* mutant did not grow on or metabolize glycerol (Table

4), further demonstrating the efficiency of this mutation. A second respiratory G3PDH (a homodimeric enzyme encoded by the *glpD* gene), which is active under aerobic conditions, has been reported to mediate glycerol respiration. Although not relevant to our study (i.e., we use anaerobic conditions), we ruled out the potential role of the a-G3PDH by demonstrating that glycerol fermentation proceeded normally in a *glpD* mutant (Table 3). The lack of a-G3PDH activity in strain Δ*glpD* was also verified through in vitro enzyme assays and by showing that this strain was unable to metabolize glycerol under aerobic conditions (Table 4). To further demonstrate the nonessential role of the respiratory pathway, we assessed glycerol fermentation in a glycerol kinase mutant (glycerol kinase is also required for the respiratory metabolism of glycerol in wild-type *E. coli* [Fig. 1]). Glycerol fermentation was still observed in the Δ*glpK* mutant (Table 3). In summary, the results presented in this section provide conclusive evidence supporting the fermentative nature of glycerol metabolism under the conditions we have reported.

Role of major fermentative pathways. In this section, we investigate the role of major fermentative pathways, namely those involved in the synthesis of ethanol, acetate, and succinate. The synthesis of acetate in *E. coli* is mediated by the *ack-pta* pathway (28). The enzyme phosphate acetyltransferase, encoded by the gene *pta*, catalyzes the conversion of acetyl coenzyme A (acetyl-CoA) to acetylphosphate, which is the first of two steps involved in this pathway (28). Inactivation of the acetate pathway in *E. coli* has been shown to be detrimental for the fermentative metabolism of some sugars. For example, Δ*pta* mutants are unable to ferment glucose or xylose (11, 28). Surprisingly, blocking acetate production did not prevent cell growth by glycerol fermentation: the Δ*pta* mutant, which produced negligible amounts of acetate, grew via glycerol fermentation in a wild-type manner (Table 3). Although in minor amounts, succinic acid is another product of glycerol fermentation (Fig. 2). We demonstrated in the previous section that the synthesis of this product is not required for glycerol fermentation: the phenotype of a Δ*frdA* mutant, which produced negligible amounts of succinic acid, was indistinguishable from that of wild-type MG1655 (Table 3).

The homoethanologenic nature of glycerol fermentation (on a molar basis, ethanol constitutes ~97% of the products found in the fermentation broth and ~92% of the fermented glycerol [Table 1]) reflects the highly reduced state of carbon in glycerol and suggests a central role for this pathway. Indeed, the synthesis of ethanol is strictly required for glycerol fermentation to proceed as no growth was observed in the Δ*adhE* mutant (Table 3). The Δ*adhE* mutant is devoid of the enzyme AdhE, which encodes an alcohol/acetaldehyde dehydrogenase responsible for the conversion of acetyl-CoA to acetaldehyde and acetaldehyde to ethanol (28). When grown in LB medium supplemented with 10 g/liter of glycerol, the Δ*adhE* mutant produced very small amounts of ethanol, providing evidence for the inactivation of alcohol/acetaldehyde dehydrogenase through the *adhE* mutation. To further support the role of AdhE, we demonstrated that the Δ*adhE* mutant recovered its ability to grow via glycerol fermentation upon complementation with a plasmid-encoded AdhE activity [Table 3; Δ*adhE* (*adhE*$^+$) strain].

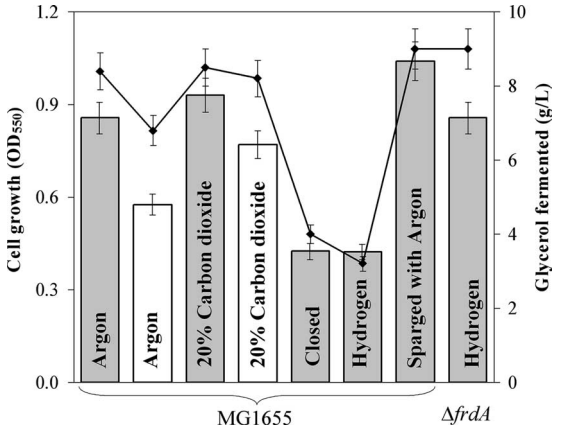

FIG. 4. Effect of pH, carbon dioxide and hydrogen on glycerol fermentation. Fermented glycerol (line) and cell growth (bars) are shown. Bar color indicates pH 6.3 (gray) or 7.5 (clear). Values represent the means and error bars represent the standard deviations for samples taken once the cultures reached stationary phase. Experiments were conducted at 37°C and using MM supplemented with 10 g/liter glycerol and 2 g/liter tryptone. The composition of the gas atmosphere is as indicated. The same results were obtained by inclusion of hydrogen as either 20% balance argon or pure hydrogen.

Effect of pH and fermentation gases on the fermentative metabolism of glycerol. We previously reported that the anaerobic metabolism of glycerol in a rich medium required an acidic pH (7). The use of low supplementation, however, allowed glycerol fermentation to proceed under alkaline conditions as well, albeit less efficiently (Fig. 4). A more detailed study of the effect of pH showed that optimum glycerol fermentation is achieved by using a pH of 6.3 (data not shown). In agreement with our previous hypothesis regarding the positive role of CO_2 on glycerol fermentation (7), a CO_2-enriched atmosphere promoted this metabolic process under both acidic and alkaline conditions (Fig. 4). In our previous study, we hypothesized that H_2, a fermentation gas coproduced along with CO_2 during the oxidation of formate, could be detrimental for glycerol fermentation (7). Supporting this hypothesis, we now show that the use of a closed vessel or the inclusion of H_2 in the gas atmosphere (the latter either as 20% H_2, balance argon, or pure hydrogen) reduced glycerol fermentation to about 50% of that observed with the use of an argon atmosphere (Fig. 4). On the other hand, continuously sparging argon through the culture medium, a condition that promotes the stripping of fermentation gases, significantly improved glycerol fermentation (Fig. 4). Interestingly, the sparged culture also exhibited a longer exponential growth phase that extended for a period of 36 h (data not shown).

To further investigate the basis of the negative effect of hydrogen on glycerol fermentation, we examined pathways involved in its metabolism. It is well known that hydrogenases mediate the utilization of hydrogen when externally provided (29). Even in the absence of external electron acceptors, the hydrogen utilized through the action of hydrogenases can be channeled to (internally generated) fumarate via the quinone pool and then readily used as an electron donor in the reduction of fumarate to succinate, a reaction catalyzed by the enzyme FRD (29). If the observed effect of hydrogen were to be

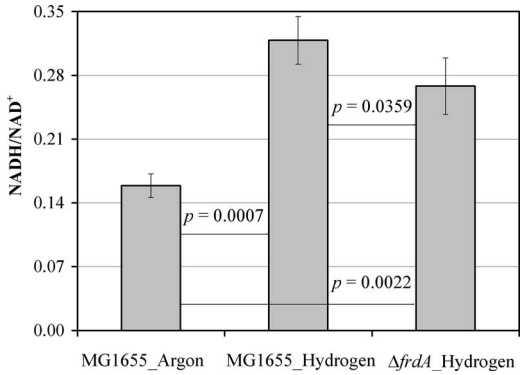

FIG. 5. Effect of gas atmosphere and hydrogen recycling on the internal redox state. The Δ*frdA* mutant is devoid of the enzyme fumarate reductase, which converts fumarate to succinate. Calculated *P* values (*t* distribution) for the comparison of the NADH/NAD$^+$ ratios are also shown.

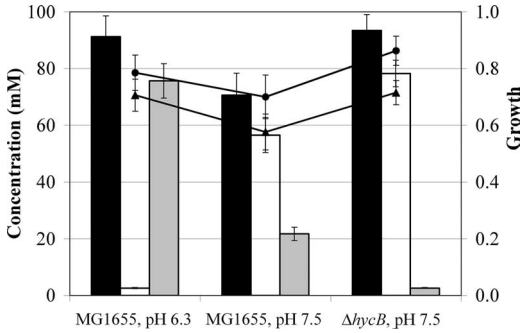

FIG. 6. Coproduction of ethanol (solid circles) and H_2 (gray bars) and ethanol (solid circles) and formic acid (clear bars) from glycerol in wild-type and engineered strains. Fermented glycerol (solid bars) and cell growth (solid triangles) are also shown. Reported values are averages of triplicate measurements, and error bars represent standard deviations. Argon was used as the headspace gas. HycB is a required component of the FHL system.

related to its utilization, as described above, it follows that mutations affecting the aforementioned process should improve cell growth and glycerol fermentation in the presence of this gas. To test this inference, we evaluated the Δ*frdA* mutant, which as reported in previous sections produces negligible amounts of succinate, indicating the lack of FRD activity. In accord with our hypothesis, blocking the FRD activity completely eliminated the negative effect of hydrogen (Fig. 4). Cell growth and glycerol fermentation in the Δ*frdA* mutant in the presence of hydrogen reached the same levels observed for MG1655 in the presence of an argon atmosphere (Fig. 4). Similar behavior was observed during growth of the Δ*frdA* mutant in a closed vessel (data not shown).

Given the highly reduced nature of carbon in glycerol and the potential impact of hydrogen recycling in the redox state of the cells (29), we characterized the internal redox state of wild-type MG1655 and the Δ*frdA* mutant in both argon and hydrogen atmospheres. To this end, we measured the intracellular NADH/NAD$^+$ ratio (see Materials and Methods for details). The inclusion of hydrogen in the gas atmosphere resulted in a twofold increase in the NADH/NAD$^+$ ratio, and a significant decrease in this parameter was observed as a result of the *frdA* mutation (Fig. 5). To demonstrate the significance of these changes, we calculated *P* values (*t* distribution) for the comparison of NADH/NAD$^+$ ratios and the results are as follows (strain/gas atmosphere compared shown in parentheses): $P = 0.0007$ (MG1655/argon versus MG1655/H_2), $P = 0.0022$ (Δ*frdA* mutant/H_2 versus MG1655/argon), and $P = 0.0359$ (Δ*frdA* mutant/H_2 versus MG1655/H_2).

Coproduction of ethanol and hydrogen or ethanol and formic acid from glycerol. When cultivated under acidic conditions (pH 6.3), wild-type strain MG1655 converts glycerol into ethanol and H_2-CO_2 almost in stoichiometric proportions (Fig. 6). Coproduction of hydrogen along with ethanol makes this process advantageous when compared to ethanol production from sugars, as the sugar-based conversion does not offer the possibility of hydrogen coproduction. Even more beneficial would be the coproduction of formic acid along with ethanol, a process that could result in the complete recovery of glycerol in these products. Since the activity of formate-hydrogen lyase (FHL), the enzyme converting formate to hydrogen and CO_2, is greatly reduced under alkaline conditions (29), we were able to achieve a significant production of formate at pH 7.5: 56 mM, compared to undetectable amounts of formate at pH 6.3 (Fig. 6). However, cell growth, glycerol fermentation, and ethanol production decreased by 10 to 20%. To further improve formate accumulation, we used a strain that contains a mutation in the *hycB* gene, which is known to be required for the activity of FHL (29). The Δ*hycB* mutant coproduced ethanol and formate in almost stoichiometric proportions and close to the maximum theoretical yield: 78 and 86 mM of formate and ethanol, respectively, were produced while glycerol consumption and cell growth were at the levels observed at pH 6.3 (Fig. 6).

DISCUSSION

Although it had been believed for many years that glycerol metabolism in *E. coli* was restricted to respiratory conditions (2, 4, 5, 15, 24, 25), we have demonstrated in this study that glycerol dissimilation in this organism can take place in a fermentative manner. Our results also indicate that the ability to anaerobically ferment glycerol is a common metabolic competency among different *E. coli* strains (Table 2). An NMR analysis of the fermentation broth allowed identifying the main fermentation products, which were further quantified via HPLC. Based on these results, we conducted a fermentation balance analysis that demonstrated an excellent closure of both carbon and redox balances. On the other hand, the analysis of the NMR spectra of proteinogenic biomass from cultures grown on U-^{13}C-labeled glycerol showed that about 20% of the carbon incorporated into the protein fraction originated from glycerol. Assuming the same percentage of incorporation of glycerol into other cellular fractions, and considering the maximum cell concentration reached by the cultures (0.4 g/liter) and the elemental composition of an *E. coli* cell (50% carbon), it follows that about 0.1 g/liter (1.1 mM) glycerol was used in the synthesis of cell mass. Since the degree of reduction per carbon in glycerol is 4.7 and that in biomass is 4.3 (cell mass formula, $CH_{1.9}O_{0.5}N_{0.2}$), a degree of reduction analysis (19)

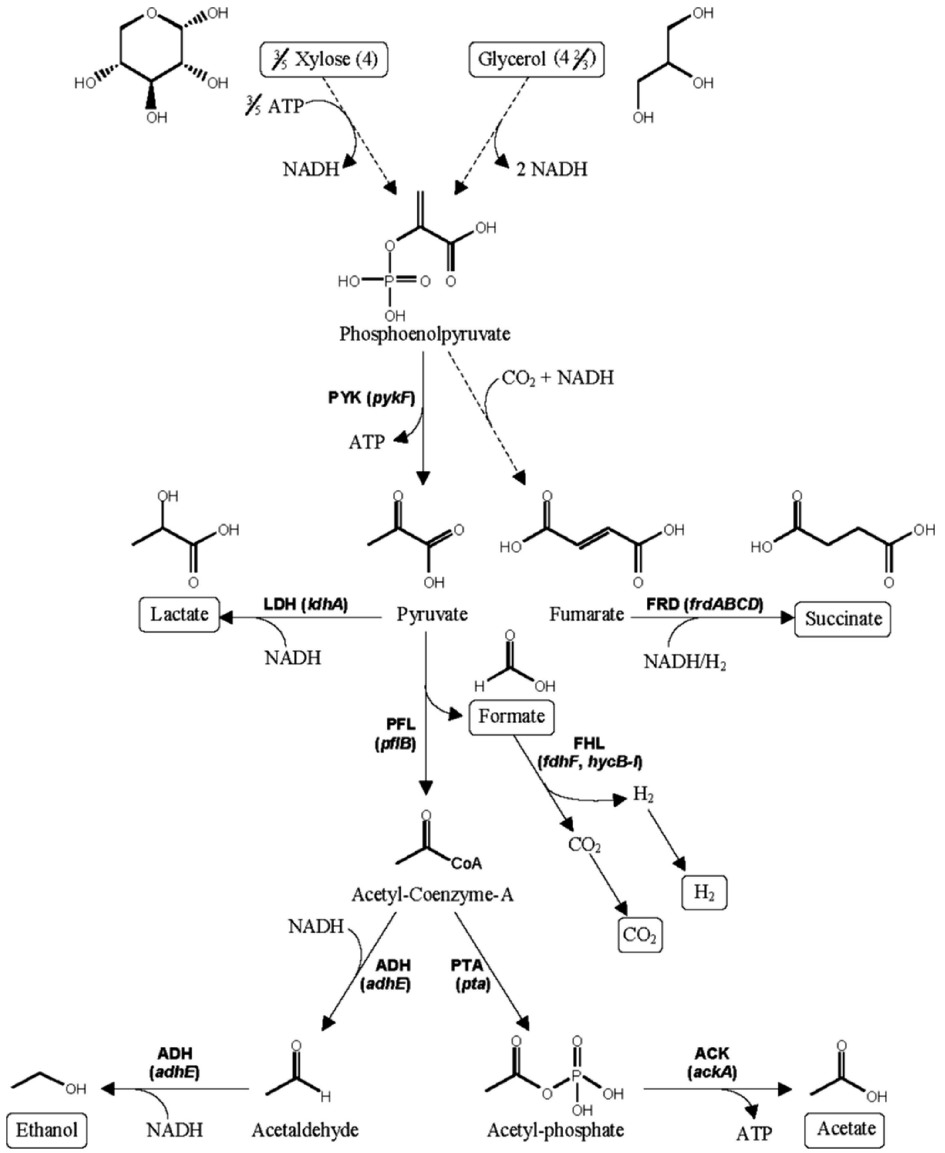

FIG. 7. Conversion of glycerol and xylose to fermentation products. The degree of reduction per carbon for xylose and glycerol is shown in parentheses and was estimated as described elsewhere (19). Enzymes catalyzing relevant steps are shown (encoding genes in parentheses). The use of NADH or H_2 as an electron donor in the reduction of fumarate to succinate involves several proteins/enzymes, including fumarate reductase, NADH dehydrogenase, hydrogenases, and menaquinones (see Fig. 8 for details). Boxed metabolites are extracellular. Abbreviations: ACK, acetate kinase; ADH, alcohol/acetaldehyde dehydrogenase; LDH, lactate dehydrogenase; PFL, pyruvate-formate lyase; PTA, phosphate acetyltransferase; and PYK, pyruvate kinase.

reveals that the incorporation of 1.1 mM glycerol into cell mass would result in the generation of about 0.6 mM reducing equivalents (e.g., 0.6 mM NADH). This excess of reducing equivalents cannot be consumed by the ethanol or succinate pathways, as the processes involved in conversion of glycerol to ethanol or succinic acid are redox-balanced processes (Fig. 7). To achieve redox balance then there must be a pathway resulting in the net consumption of reducing equivalents. The synthesis of 1,2-PDO ($C_3H_8O_2$; degree of reduction per carbon, 5.33) from glycerol ($C_3H_8O_3$) could provide such a pathway, which would consume as much as 1 mol of reducing equivalent per mol of 1,2-PDO synthesized. Interestingly, we identified a doublet in the NMR spectra of fermentation samples at the same position of 1,2-PDO methyl protons (Fig. 2A, inset I) and which we estimated to correspond to about 0.5 mM 1,2-PDO. Therefore, the synthesis of this amount of 1,2-PDO would be sufficient to provide a sink for the reducing equivalents generated in the synthesis of cell mass (about 0.6 mM NADH).

The almost exclusive synthesis of reduced product ethanol (Fig. 2A) was interpreted as a strong indication that glycerol is in fact metabolized in a fermentative manner: i.e., the presence of an electron acceptor would otherwise consume the reducing equivalents generated from glycerol and significant amounts of oxidized products (such as acetate) would be produced instead of ethanol. More direct evidence of the fermentative nature of glycerol metabolism was provided in studies in which cell

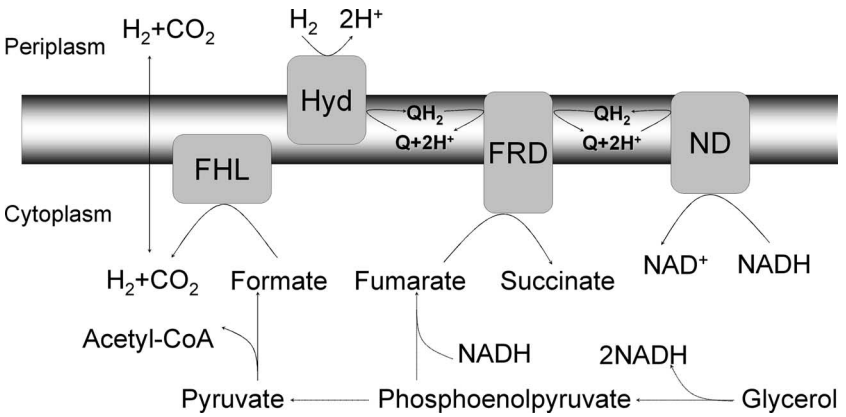

FIG. 8. Generation and recycling of hydrogen and their relationship to succinate production during the fermentative metabolism of glycerol. The use of hydrogen as an electron donor in the reduction of fumarate makes the conversion of glycerol to succinate a "redox-generating" pathway. See Fig. 7 for details about ATP use/generation in these pathways. Abbreviations: Hyd, hydrogenases I and II; ND, NADH dehydrogenase; and Q, quinone pool.

growth and glycerol utilization were still observed despite blocking several respiratory processes (Table 3). Of special relevance is the observation that mutants devoid of key enzymes involved in the respiratory metabolism of glycerol were able to metabolize this carbon source. The latter not only provides conclusive evidence supporting the fermentative nature of this process but also indicates the existence of alternative pathways for the fermentative dissimilation of glycerol. In other studies, currently under way in our laboratory, we have demonstrated that this alternative pathway is composed of a type II glycerol dehydrogenase (*gldA*) and a phosphoenolpyruvate-dependent dihydroxyacetone kinase (*dhaKLM*) (Gonzalez et al., unpublished data).

Major determinants of the fermentative metabolism of glycerol: metabolic and environmental factors. While the synthesis of acetate is required for the fermentation of sugars such as glucose and xylose (11, 28), this metabolic pathway is nonessential during the fermentative metabolism of glycerol (Table 3). The synthesis of ethanol, however, was an absolute requirement for glycerol fermentation to proceed (Table 3). Further inspection of the major pathways active during the fermentation of glycerol reveals that the synthesis of ethanol is the only pathway that can perform the two major functions that determine the fermentative metabolism of a given carbon source, namely attaining redox balance and generation of ATP via substrate-level phosphorylation (Fig. 7). The operation of the ethanologenic pathway results in the net production of 1 ATP per glycerol metabolized (Fig. 7), which favorably compares with the ATP yield obtained by fermentation of other sugars. For example, considering the constraints imposed by the overall redox balance, only 0.9 ATP is generated during the fermentative metabolism of xylose (three-carbon basis) (Fig. 7). While conversion of glycerol to succinate is also a redox-balanced pathway, its contribution to ATP generation is very limited (34). Perhaps this is the reason why very small amounts of succinate are synthesized during the fermentation of glycerol (Fig. 2A) and no significant effect is observed when the conversion of fumarate to succinate is blocked (Table 3). We then conclude that the ethanologenic pathway is a metabolic determinant of glycerol fermentation as it ensures the generation of ATP through a redox-balanced process in the absence of electron acceptors.

A key environmental determinant for the fermentative metabolism of glycerol is the use of conditions that prevent the accumulation of fermentation gas hydrogen (Fig. 4). We demonstrated that the negative effect of hydrogen is related to the reduction of fumarate to succinate, as a strain devoid of the enzyme FRD was not affected by the presence of this gas (Fig. 4). We also showed that inclusion of hydrogen resulted in a 2-fold increase in the NADH/NAD^+ ratio in MG1655 compared to only a 1.6-fold change in the Δ*frdA* mutant (Fig. 5). During glycerol fermentation in the absence of externally provided hydrogen (e.g., argon/nitrogen atmosphere or a closed vessel), this gas is generated by the disproportionation of formate into CO_2 and H_2, a reaction catalyzed by the enzymatic complex FHL (28, 29) (Fig. 7 and 8). It has also been shown that under fermentative conditions, hydrogenase isoenzyme 1 (Hyd-1) or 2 (Hyd-2) can serve the function of recycling the hydrogen evolved by the FHL complex (6, 27, 29, 30). Based on our results, we propose that hydrogen recycling takes place during glycerol fermentation and that this gas is used as electron donor in the conversion of fumarate to succinate (Fig. 8). Considering that the conversion of glycerol to succinate is already a redox-balanced process, the use of hydrogen as an electron donor creates an excess of reducing equivalents (Fig. 8). The latter could then result in a redox imbalance, as this excess of reducing equivalents cannot be consumed by any of the other fermentative pathways: i.e., none of the main pathways active during glycerol fermentation represents a "sink" of reducing equivalents (Fig. 7). Our characterization of internal redox state accords with this idea as the estimated NADH/NAD^+ ratio increased by twofold due to the inclusion of hydrogen (Fig. 5). Moreover, the Δ*frdA* mutant exhibited an NADH/NAD^+ ratio in a hydrogen atmosphere that was about 20% lower than that found in the MG1655 culture under the same conditions. Taken together, these results clearly demonstrate that the negative effect of hydrogen is due to its recycling and use as electron donor in the reduction of fumarate, a process that ultimately leads to a significant redox imbalance (Fig. 8).

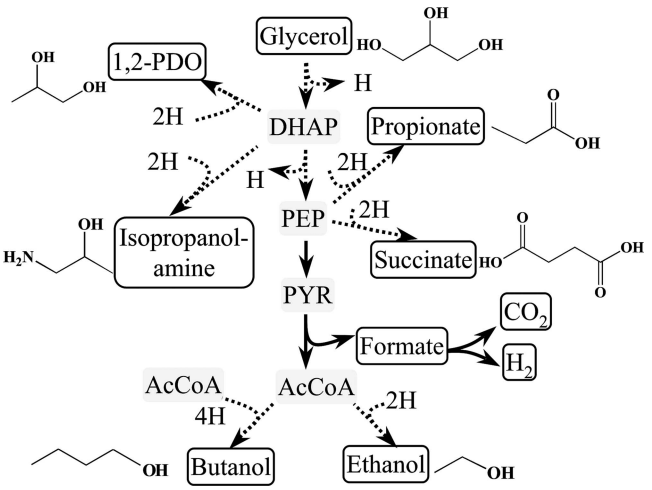

FIG. 9. Anaerobic fermentation of glycerol as a platform for the production of fuels and reduced chemicals. Synthesis of these products from glycerol is a redox-balanced or redox-consuming process. The synthesis of ethanol or butanol along with either CO_2-H_2 or formate would generate ATP. Engineering the remaining pathways would involve their transformation to either ATP-generating (succinate and propionate) or ATP-neutral (1,2-PDO and isopropanolamine) pathways. The maximum theoretical yield in each case is higher than that possible from the use of common sugars such as glucose or xylose. The butanol pathway is not native in *E. coli*. Abbreviations: AcCoA, acetyl-CoA; DHAP, dihydroxyacetone phosphate; PEP, phosphoenolpyruvate; PYR, pyruvate; and 1,2-PDO, 1,2-propanediol.

Accumulation of hydrogen, and therefore creation of a redox imbalance, could be one of the reasons why the fermentative metabolism of glycerol in *E. coli* was not previously observed. Cultivation systems often employed to study the fermentative behavior of an organism include the use of closed flasks/tubes completely filled with medium (e.g., Hungate tubes as described in Materials and Methods). Indeed, we tested such system (Hungate tubes with no headspace) and found that glycerol fermentation by MG1655 was significantly impaired. However, substantial fermentation of glycerol was observed in the Δ*frdA* mutant, which we have shown avoids the negative impact of hydrogen by maintaining appropriate redox conditions (Fig. 4 and 5). These results further support our conclusion that recycling of molecular hydrogen evolved by the FHL complex and its use as electron donor in the reduction of fumarate result in a redox imbalance that negatively affects glycerol fermentation (Fig. 8).

Fermentative utilization of glycerol in *E. coli* as a new path to biofuels and biochemicals. The conversion of low-priced glycerol streams to higher value products has been proposed as a path to economic viability for the biofuels industry (38). Crude glycerol is an inevitable by-product of biodiesel production, and has become an attractive carbon source for fermentation processes because of its low price and availability. Given the higher reduced state of carbon in glycerol compared to sugars traditionally used in fermentation processes (e.g., the degree of reduction per carbon for glucose and xylose is 4 compared to 4.67 for glycerol [Fig. 7]), the use of glycerol as substrate in the production of fuels and reduced chemicals is very promising (38). This advantage becomes even more significant when the industrial organism *E. coli*, which is considered to be the workhorse of modern biotechnology, is used as the biocatalyst. Since the feasibility of engineering *E. coli* for the production of chemicals and fuels has been extensively documented (10, 37), our findings will enable the use of metabolic engineering strategies to develop *E. coli*-based platforms for the anaerobic production of reduced chemicals from glycerol at yields higher than those obtained from common sugars. Figure 9 presents some examples in which product yields would be greatly enhanced by the use of glycerol. Our initial results for the coproduction of ethanol H_2 and CO_2 and coproduction of ethanol and formic acid were discussed in this paper (see Fig. 6). The development of processes for the production of these chemicals and fuels would enable the implementation of true biorefineries and revolutionize the biofuels industry by greatly improving its economics.

ACKNOWLEDGMENTS

This work was supported by grants from the National Research Initiative of the U.S. Department of Agriculture Cooperative State Research, Education and Extension Service (2005-35504-16698) and the U.S. National Science Foundation (CBET-0645188).

We thank F. R. Blattner and H. Mori for providing research materials, S. Moran and E. Nikonowicz for assistance with NMR experiments, and K.-Y. San for assistance with the NADH/NAD^+ assay.

REFERENCES

1. **Bax, A.** 1983. A simple method for the calibration of the decoupler radio-frequency field-strength. J. Magn. Res. **52:**76–80.
2. **Booth, I. R.** March 2005, posting date. Chapter 3.4.3, Glycerol and methylglyoxal metabolism. *In* R. Curtis III et al. (ed.), EcoSal—*Escherichia coli* and *Salmonella*: cellular and molecular biology. ASM Press, Washington, DC. http://www.ecosal.org.
3. **Borgnia, M. J., and P. Agre.** 2001. Reconstitution and functional comparison of purified GlpF and AqpZ, the glycerol and water channels from *Escherichia coli*. Proc. Natl. Acad. Sci. USA **98:**2888–2893.
4. **Bouvet, O. M. M., P. Lenormand, E. Ageron, and P. A. D. Grimont.** 1995. Taxonomic diversity of anaerobic glycerol dissimilation in the *Enterobacteriaceae*. Res. Microbiol. **146:**279–290.
5. **Bouvet, O. M. M., P. Lenormand, J. P. Carlier, and P. A. D. Grimont.** 1994. Phenotypic diversity of anaerobic glycerol dissimilation shown by 7 enterobacterial species. Res. Microbiol. **145:**129–139.
6. **Clark, D. P.** 1989. The fermentation pathways of *Escherichia coli*. FEMS Microbiol. Rev. **63:**223–234.
7. **Dharmadi, Y., A. Murarka, and R. Gonzalez.** 2006. Anaerobic fermentation of glycerol by *Escherichia coli*: a new platform for metabolic engineering. Biotechnol. Bioeng. **94:**821–829.
8. **Dharmadi, Y., and R. Gonzalez.** 2005. A better global resolution function and a novel iterative stochastic search method for optimization of high-performance liquid chromatographic separation. J. Chromatogr. A **1070:**89–101.
9. **Fan, W. M. T.** 1996. Metabolite profiling by one- and two-dimensional NMR analysis of complex mixtures. Prog. NMR Spectrosc. **28:**161–219.
10. **Gonzalez, R.** 2005. Metabolic engineering of bacteria for food ingredients, p. 111–130. *In* K. Shetty, G. Paliyath, A. Pometto, and R. E. Levin (ed.), Food biotechnology, 2nd ed. CRC Press, Boca Raton, FL.
11. **Hasona, A., Y. Kim, F. G. Healy, L. O. Ingram, and K. T. Shanmugam.** 2004. Pyruvate formate lyase and acetate kinase are essential for anaerobic growth of *Escherichia coli* on xylose. J. Bacteriol. **186:**7593–7600.
12. **Kang, Y., T. Durfee, J. D. Glasner, Y. Qiu, D. Frisch, K. M. Winterberg, and F. R. Blattner.** 2004. Systematic mutagenesis of the *Escherichia coli* genome. J. Bacteriol. **186:**4921–4930.
13. **Kistler, W. S., and E. C. C. Lin.** 1972. Purification and properties of the flavine-stimulated anaerobic L-α-glycerophosphate dehydrogenase of *Escherichia coli*. J. Bacteriol. **112:**539–547.
14. **Kitagawa, M., T. Ara, M. Arifuzzaman, T. Ioka-Nakamichi, E. Inamoto, H. Toyonaga, and H. Mori.** 2005. Complete set of ORF clones of *Escherichia coli* ASKA library (A complete Set of *E. coli* K-12 ORF Archive): unique resources for biological research. DNA Res. **12:**291–299.
15. **Lin, E. C. C.** 1976. Glycerol dissimilation and its regulation in bacteria. Annu. Rev. Microbiol. **30:**535–578.
16. **McCoy, M.** 2005. An unlikely impact. Chem. Eng. News **83:**24–26.
17. **McCoy, M.** 2006. Glycerin surplus. Chem. Eng. News **84:**7–8.
18. **Neidhardt, F. C., P. L. Bloch, and D. F. Smith.** 1974. Culture medium for enterobacteria. J. Bacteriol. **119:**736–747.

19. **Nielsen, J., J. Villadsen, and G. Liden.** 2003. Bioreaction engineering principles, p. 60–73. Kluwer Academic/Plenum Publishers, New York, NY.
20. **Osman, Y. A., T. Conway, S. J. Bonetti, and L. O. Ingram.** 1987. Glycolytic flux in *Zymomonas mobilis*: enzyme and metabolite levels during batch fermentation. J. Bacteriol. **169:**3726–3736.
21. **Peters, J. E., T. E. Thate, and N. L. Craig.** 2003. Definition of the *Escherichia coli* MC4100 genome by use of a DNA array. J. Bacteriol. **185:**2017–2021.
22. **Pettigrew, D. W., G. J. Yu, and Y. G. Liu.** 1990. Nucleotide regulation of *Escherichia coli* glycerol kinase—initial velocity and substrate binding studies. Biochemistry **29:**8620–8627.
23. **Phue, J. N., and J. Shiloach.** 2004. Transcription levels of key metabolic genes are the cause for different glucose utilization pathways in *E. coli* B (BL21) and *E. coli* K (JM109). J. Biotechnol. **109:**21–30.
24. **Quastel, J. H., and M. Stephenson.** 1925. Further observations on the anaerobic growth of bacteria. Biochem. J. **19:**660–666.
25. **Quastel, J. H., M. Stephenson, and M. D. Whetham.** 1925. Some reactions of resting bacteria in relation to anaerobic growth. Biochem. J. **19:**304–317.
26. **Sambrook, J., E. F. Fritsch, and T. Maniatis.** 1989. Molecular cloning: a laboratory manual, 2nd ed. Cold Spring Harbor Laboratory Press, Cold Spring Harbor, NY.
27. **Sawers, R. G., and D. H. Boxer.** 1986. Purification and properties of membrane-bound hydrogenase isoenzyme 1 from anaerobically grown *Escherichia coli* K12. Eur. J. Biochem. **156:**265–275.
28. **Sawers, R. G., and D. P. Clark.** July 2004, posting date. Chapter 3.5.3, Fermentative pyruvate and acetyl-coenzyme A metabolism. *In* R. Curtis III et al. (ed.), EcoSal—*Escherichia coli* and *Salmonella*: cellular and molecular biology. ASM Press, Washington, DC. http://www.ecosal.org.
29. **Sawers, R. G., M. Blokesch, and A. Böck.** September 2004, posting date. Chapter 3.5.4, Anaerobic formate and hydrogen metabolism. *In* R. Curtis III et al. (ed.), EcoSal—*Escherichia coli* and *Salmonella*: cellular and molecular biology. ASM Press, Washington, DC. http://www.ecosal.org.
30. **Sawers, R. G., S. P. Ballantine, and D. H. Boxer.** 1985. Differential expression of hydrogenase isoenzymes in *Escherichia coli* K-12: evidence for a third isoenzyme. J. Bacteriol. **164:**1324–1331.
31. **Schryvers, A., and J. H. Weiner.** 1982. The anaerobic *sn*-glycerol-3-phosphate dehydrogenase—cloning and expression of the *glpA* gene of *Escherichia coli* and identification of the *glpA* products. Can. J. Biochem. **60:**224–231.
32. **Shalel-Levanon, S., K. Y. San, and G. N. Bennett.** 2005. Effect of ArcA and FNR on the expression of genes related to the oxygen regulation and the glycolysis pathway in *Escherichia coli* under microaerobic growth conditions. Biotechnol. Bioeng. **92:**147–159.
33. **Tao, H., R. Gonzalez, A. Martinez, M. Rodriguez, L. O. Ingram, J. F. Preston, and K. T. Shanmugam.** 2001. Engineering a homo-ethanol pathway in *Escherichia coli*: increased glycolytic flux and levels of expression of glycolytic genes during xylose fermentation. J. Bacteriol. **183:**2979–2988.
34. **Unden, G., and A. Kleefield.** July 2004, posting date. Chapter 3.4.5, C_4-dicarboxylate degradation in aerobic and anaerobic growth. *In* R. Curtis III et al. (ed.), EcoSal—*Escherichia coli* and *Salmonella*: cellular and molecular biology. ASM Press, Washington, DC. http://www.ecosal.org.
35. **Walt, A., and M. L. Kahn.** 2002. The *fixA* and *fixB* genes are necessary for anaerobic carnitine reduction in *Escherichia coli*. J. Bacteriol. **184:**4044–4047.
36. **Walz, A. C., R. A. Demel, B. de Kruijff, and R. Mutzel.** 2002. Aerobic sn-glycerol-3-phosphate dehydrogenase from *Escherichia coli* binds to the cytoplasmic membrane through an amphipathic alpha-helix. Biochem. J. **365:**471–479.
37. **Wendisch, V. F., M. Bott, and B. J. Eikmanns.** 2006. Metabolic engineering of *Escherichia coli* and *Corynebacterium glutamicum* for biotechnological production of organic acids and amino acids. Curr. Opin. Microbiol. **9:**268–274.
38. **Yazdani, S. S., and R. Gonzalez.** 2007. Anaerobic fermentation of glycerol: a path to economic viability for the biofuels industry. Curr. Opin. Biotechnol. **18:**213–219.